Spin Contamination Error in Optimized Geometry of Singlet Carbene ($^1A_1$) by Broken-Symmetry Method†

Yasutaka Kitagawa,* Toru Saito, Yasuyuki Nakanishi, Yusuke Kataoka, Toru Matsui, Takashi Kawakami, Mitsutaka Okumura, and Kizashi Yamaguchi

Department of Chemistry, Graduate School of Science, Osaka University, 1-1 Machikaneyama, Toyonaka, Osaka 560-0043, Japan

Received: June 1, 2009; Revised Manuscript Received: September 21, 2009

Spin contamination errors of a broken-symmetry (BS) method in optimized structural parameters of the singlet methylene ($^1A_1$) molecule are quantitatively estimated for the Hartree−Fock (HF) method, post-HF methods (CID, CCD, MP2, MP3, MP4(SDQ)), and a hybrid DFT (B3LYP) method. For the purpose, the optimized geometry by the BS method is compared with that of an approximate spin projection (AP) method. The difference between the BS and the AP methods is about 10−20° in the HCH angle. In order to examine the basis set dependency of the spin contamination error, calculated results by STO-3G, 6-31G*, and 6-311++G** are compared. The error depends on the basis sets, but the tendencies of each method are classified into two types. Calculated energy splitting values between the triplet and the singlet states (ST gap) indicate that the contamination of the stable triplet state makes the BS singlet solution stable and the ST gap becomes small. The energy order of the spin contamination error in the ST gap is estimated to be 10^{-1} eV.

1. Introduction

A reproduction of experimental molecular structures and an expectation of undiscovered ones are one of the long-cherished hopes of quantum chemists. For small systems, *accurate* structures will be calculated by *accurate* wave functions;[1] however one must introduce some approximations for larger systems. Recent progress in ab initio and density functional theory (DFT) methods has enabled us to calculate geometries of large molecules with accelerated CPUs. For example, there have been some reports that theoretical calculations have settled problems in experiments.[2,3] Those compounds often involve energetically quasi-degenerate orbitals that cause a static (nondynamical) correlation effect.[4,5] Complete active space (CAS)[6,7] and multireference (MR)[8] methods are the straightforward ways to include a correction of the static correlation; however those methods often cannot be applied to the larger systems because of the high cost of computation. One of the alternatives is a broken-symmetry (BS) method, which corrects the static correlation approximately at the lower cost of computation.[9-12] The BS method such as unrestricted Hartree−Fock (UHF) and unrestricted DFT (UDFT) allows a spin-symmetry breaking and approximates the static correlation correction by splitting α and β electrons into two different orbitals, namely, different orbitals for different spins (DODS) approach.[13,14] Because of its low computational cost, the BS method is widely used for theoretical geometry optimization of the large systems. On the BS method, a singlet spin state with the strong static correlation is expressed as a singlet biradical. In those singlet biradicals of the BS method, there is a serious problem called a spin contamination error that higher spin states are involved in the singlet wave function.[15-19] The influence of the spin contamination appears everywhere, such as total energy, optimized geometry, excited energy, and so on, because it originates in the BS wave function itself.

For the calculation of a molecular geometry and some properties, an energy derivative is necessary. For example, the first energy derivative, i.e., the energy gradient, is required for the calculations of the molecular structure. And the second energy derivative, i.e., Hessian, is also widely used for the calculations of IR frequency, geometry optimizations for ground and transition states, and so on.[20] Therefore a quantitative calculation of the energy derivatives is an important subject for the theoretical and computational chemistry in a molecular science.

From above points of view, the elimination of the spin contamination error in the energy derivatives is indispensable for the accurate calculations of molecular geometries and some properties. However an investigation about the spin contamination error in the energy derivatives of the BS method has been still insufficient. Recently our group has proposed a new method to eliminate the spin contamination error from the energy gradient and Hessian based on Yamaguchi's approximate spin projection (AP) procedure.[21-23] We have utilized the AP gradient for the geometry optimization (AP-opt) so that the geometry of biradical molecules can be optimized without the spin contamination error.[24]

In this paper, we apply the AP-opt method to the singlet methylene (($^1A_1$), which is one of the typical singlet biradicals, and demonstrate that the spin contamination strongly affects to the optimized geometry. The effect of the spin contamination in the singlet−triplet energy splitting (S-T gap) is also examined by using the calculated results.

2. Theoretical Background

In this section, a theoretical background of the AP method is explained by starting from the simplest two-orbital and two-spin model such as the singlet CH_2 illustrated in Figure 1a. Two

† Part of the "Vincenzo Aquilanti Festschrift".

* To whom correspondence should be addressed. Tel: (+81) 6-6850-5405. Fax: (+81) 6-6850-5550. E-mail: kitagawa@chem.sci.osaka-u.ac.jp.

10.1021/jp905125g
Published on Web 10/09/2009

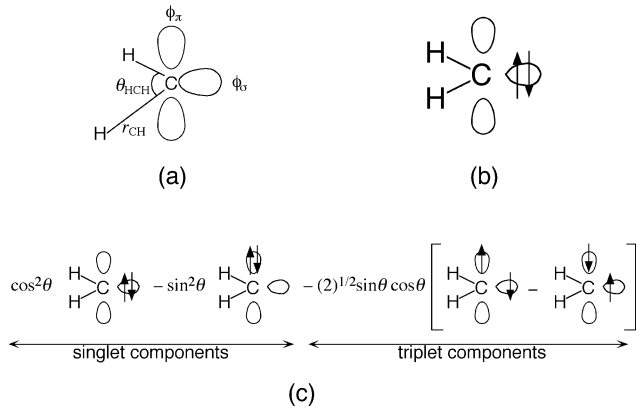

Figure 1. (a) Structure and two quasi-degenerate orbitals (ϕ_σ and ϕ_π) of methylene. Schematic representations of the electron configurations of (b) the SA (restricted) and (c) the BS methods.

valence orbitals of the carbene are constructed by ϕ_σ and ϕ_π orbitals.[5] The BS (DODS) singlet state of $^1A_1$ is usually obtained from a mix of those two orbitals. This procedure is quite similar to H_2 molecule. For example, two electrons of the H_2 molecule are both in a same σ orbital at an equilibrium distance (H$\uparrow\downarrow$H). We call this electronic state a spin-symmetry adapted (SA) (or closed shell) state. However, those two electrons are separated into two localized atomic orbitals at a dissociation limit ($\uparrow$H$\cdots$H$\downarrow$) by the HOMO−LUMO mixing. Two HOMO orbitals of H_2, i.e., alpha (ψ_σ^α) and beta (ψ_σ^β) orbitals of the BS method are expressed as follows

$$\psi_\sigma^\alpha = \cos\theta\phi_\sigma + \sin\theta\phi_\sigma^* \quad (1)$$

$$\psi_\sigma^\beta = \cos\theta\phi_\sigma - \sin\theta\phi_\sigma^* \quad (2)$$

where ϕ_σ and ϕ_σ^* express HOMO and LUMO orbitals of SA (or restricted (R)) calculations, respectively,[13,14] θ is a mixing parameter, which ranges $0 \le \theta \le \pi/4$. When θ is not zero, the spatial orbitals of α and β electrons are different from each other ($\psi_\sigma^\alpha \neq \psi_\sigma^\beta$), in other words, the spin-symmetry is broken. This situation is specifically called the unrestricted broken-symmetry (U-BS) state (or singlet biradical state). We note that the U-BS state is often simply called the "unrestricted" or "BS" state. The wave function of the U-BS singlet is

$$|\Psi_{\text{U-BS}}^{\text{Singlet}}\rangle = \cos^2\theta|\phi_\sigma\bar{\phi}_\sigma\rangle - \sin^2\theta|\phi_\sigma^*\bar{\phi}_\sigma^*\rangle - \sqrt{2}\cos\theta\sin\theta|\Psi^{\text{Triplet}}\rangle \quad (3)$$

where ϕ_σ and $\bar{\phi}_\sigma$ express α and β electrons in orbital ϕ_σ, respectively. In this way, the orbital mixing leads a contamination of higher spin states in a singlet wave function. The U-BS wave function causes α and β spin densities and gives nonzero $\langle\hat{\mathbf{S}}^2\rangle_{\text{U-BS}}^{\text{Singlet}}$ value. We often regard such spin densities as existing of localized spins. An interaction between the localized spins can be expressed by Heisenberg Hamiltonian,

$$\hat{\mathbf{H}}_{\text{H}} = -2\sum_{a<b} J_{ab}\hat{\mathbf{S}}_a \cdot \hat{\mathbf{S}}_b \quad (4)$$

where $\hat{\mathbf{S}}_a$ and $\hat{\mathbf{S}}_b$ are spin operators for spin sites a and b, respectively, and J_{ab} is an effective exchange integral.[11,12] Using a total spin operator of the system $\hat{\mathbf{S}} = \hat{\mathbf{S}}_a + \hat{\mathbf{S}}_b$, eq 4 becomes

$$\hat{\mathbf{H}}_{\text{H}} = \sum_{a<b} J_{ab}(-\hat{\mathbf{S}}^2 + \hat{\mathbf{S}}_a^2 + \hat{\mathbf{S}}_b^2) \quad (5)$$

Multiplying Hamitonian of eq 5 to eq 3, then the singlet state energy in the Heisenberg Hamiltonian ($E_{\text{H}}^{\text{Singlet}}$) is expressed as

$$E_{\text{H}}^{\text{singlet}} = J_{ab}(-\langle\hat{\mathbf{S}}^2\rangle^{\text{singlet}} + \langle\hat{\mathbf{S}}_a^2\rangle^{\text{singlet}} + \langle\hat{\mathbf{S}}_b^2\rangle^{\text{singlet}}) \quad (6)$$

Similarly, for the triplet state

$$E_{\text{H}}^{\text{Triplet}} = J_{ab}(-\langle\hat{\mathbf{S}}^2\rangle^{\text{Triplet}} + \langle\hat{\mathbf{S}}_a^2\rangle^{\text{Triplet}} + \langle\hat{\mathbf{S}}_b^2\rangle^{\text{Triplet}}) \quad (7)$$

The energy difference of the ab initio method between singlet and triplet states can be projected to the energy difference between $E_{\text{H}}^{\text{Singlet}}$ and $E_{\text{H}}^{\text{Triplet}}$. And if we can assume that $\langle\hat{\mathbf{S}}_i^2\rangle$ values of the U-BS singlet state at spin site i ($i = a$ or b) are almost equal to those of the triplet state, i.e., $\langle\hat{\mathbf{S}}_i^2\rangle_{\text{U}}^{\text{Triplet}} \cong \langle\hat{\mathbf{S}}_i^2\rangle_{\text{U-BS}}^{\text{Singlet}}$, then J_{ab} can be derived as

$$J_{ab} = \frac{E_{\text{H}}^{\text{singlet}} - E_{\text{H}}^{\text{Triplet}}}{(\langle\hat{\mathbf{S}}^2\rangle_{\text{H}}^{\text{Triplet}} - \langle\hat{\mathbf{S}}^2\rangle_{\text{H}}^{\text{singlet}})} = \frac{E_{\text{U-BS}}^{\text{singlet}} - E_{\text{U}}^{\text{Triplet}}}{(\langle\hat{\mathbf{S}}^2\rangle_{\text{U}}^{\text{Triplet}} - \langle\hat{\mathbf{S}}^2\rangle_{\text{U-BS}}^{\text{singlet}})} \quad (8)$$

Here, we use subscript "U" for the triplet state specifically in order to distinguish a conventional "unrestricted" method from a "restricted-open shell (RO)" method. If the method is exact and the spin contamination in both singlet and triplet states is zero (i.e $\langle\hat{\mathbf{S}}^2\rangle_{\text{exact}}^{\text{Singlet}} = 0$ and $\langle\hat{\mathbf{S}}^2\rangle_{\text{exact}}^{\text{Triplet}} = S_{\max}(S_{\max}+1)$, where $S_{\max} = S_a + S_b$), the energy gap between singlet and triplet states must be equal to $2J_{ab}$ as

$$E_{\text{exact}}^{\text{Singlet}} - E_{\text{exact}}^{\text{Triplet}} = 2J_{ab} \quad (9)$$

However the spin contamination in the triplet state is usually negligible (i.e., $\langle\hat{\mathbf{S}}^2\rangle_{\text{U}}^{\text{Triplet}} \cong S_{\max}(S_{\max}+1) = 2$) but not in the U-BS state, so that the energy gap becomes

$$E_{\text{U-BS}}^{\text{singlet}} - E_{\text{U}}^{\text{Triplet}} = 2J_{ab} - J_{ab}\langle\hat{\mathbf{S}}^2\rangle_{\text{U-BS}}^{\text{singlet}} \quad (10)$$

Equation 10 means that a second term in a denominator of eq 8 corrects the spin contamination error in the U-BS solution. In this way, eq 8 gives the spin-projected J_{ab} value. It can be easily expanded into any spin dimers, namely, the lowest spin state (LS) and the highest spin state (HS), e.g., singlet−quintet for $S_a = S_b = 2/2$ pairs and singlet−sextet for $S_a = S_b = 3/2$ pairs, as follows

$$J_{ab} = \frac{E_{\text{U-BS}}^{\text{LS}} - E_{\text{U}}^{\text{HS}}}{(\langle\hat{\mathbf{S}}^2\rangle_{\text{U}}^{\text{HS}} - \langle\hat{\mathbf{S}}^2\rangle_{\text{U-BS}}^{\text{LS}})} \quad (11)$$

The eq 11 is the so-called Yamaguchi formula to calculate J_{ab} values with the AP procedure.[11,12] Because J_{ab} calculated by eq 11 is a value that the spin contamination error has approximately eliminated, it should be equal to the J_{ab} value calculated by the approximate spin-projected wave functions, namely

$$J_{ab} = \frac{E^{LS}_{U\text{-}BS} - E^{HS}_{U}}{\langle \hat{S}^2 \rangle^{HS}_{U} - \langle \hat{S}^2 \rangle^{LS}_{U\text{-}BS}} = \frac{E^{LS}_{AP\text{-}BS} - E^{HS}_{AP\text{-}U}}{\langle \hat{S}^2 \rangle^{HS}_{exact} - \langle \hat{S}^2 \rangle^{LS}_{exact}} \quad (12)$$

where $E^{LS}_{AP\text{-}BS}$ and $E^{HS}_{AP\text{-}U}$ are spin-projected total energies of the HS and the LS states, respectively. Here, the spin contamination in the HS state is usually negligible, i.e.

$$\langle \hat{S}^2 \rangle^{HS}_{U} \cong \langle \hat{S}^2 \rangle^{HS}_{exact} \quad \text{and} \quad E^{HS}_{U} \cong E^{HS}_{AP\text{-}U} \quad (13)$$

then one can obtain a spin projected energy of the singlet state without the spin contamination as follows[17,18]

$$E^{LS}_{AP\text{-}BS} = \alpha E^{LS}_{U\text{-}BS} - \beta E^{HS}_{U} \quad (14)$$

where

$$\alpha = \frac{\langle \hat{S}^2 \rangle^{HS}_{U} - \langle \hat{S}^2 \rangle^{LS}_{exact}}{\langle \hat{S}^2 \rangle^{HS}_{U} - \langle \hat{S}^2 \rangle^{LS}_{U\text{-}BS}} \quad (15)$$

$$\beta = \frac{\langle \hat{S}^2 \rangle^{LS}_{U\text{-}BS} - \langle \hat{S}^2 \rangle^{LS}_{exact}}{\langle \hat{S}^2 \rangle^{HS}_{U} - \langle \hat{S}^2 \rangle^{LS}_{U\text{-}BS}} \quad (16)$$

$$\beta = \alpha - 1 \quad (17)$$

This is the AP energy for the U-BS singlet state based on Yamaguchi's formula.

$E^{LS}_{AP\text{-}BS}$ can be expanded by using Taylor series

$$E^{LS}_{AP\text{-}BS}(\boldsymbol{R}^{LS}_{AP\text{-}BS}) = E^{LS}_{AP\text{-}BS}(\boldsymbol{R}) + \boldsymbol{X}^{T}\boldsymbol{G}^{LS}_{AP\text{-}BS}(\boldsymbol{R}) + \frac{1}{2}\boldsymbol{X}^{T}\boldsymbol{F}^{LS}_{AP\text{-}BS}(\boldsymbol{R})\boldsymbol{X} + \cdots \quad (18)$$

where $\mathbf{G}^{LS}_{AP\text{-}BS}(\mathbf{R})$ and $\mathbf{F}^{LS}_{AP\text{-}BS}(\mathbf{R})$ are the spin projected energy gradient (AP gradient) and the spin projected Hessian (AP Hessian), respectively.[21-23] Here, $\mathbf{R}^{LS}_{AP\text{-}BS}$, $\mathbf{R}$, and $\mathbf{X}$ are the stationary point of $E^{LS}_{AP\text{-}BS}(\mathbf{R})$, the present position, and the position vector ($\mathbf{R}^{LS}_{AP\text{-}BS} - \mathbf{R}$), respectively. From eqs 14−17, we obtain the AP gradient and the AP Hessian for the U-BS state as follows,

$$\mathbf{G}^{LS}_{AP\text{-}BS}(\mathbf{R}) = \frac{\partial E^{LS}_{AP\text{-}BS}(\mathbf{R})}{\partial \mathbf{R}} = \{\alpha(\mathbf{R})\mathbf{G}^{LS}_{U\text{-}BS}(\mathbf{R}) - \beta(\mathbf{R})\boldsymbol{G}^{HS}_{U}(\mathbf{R})\} + \frac{\partial \alpha(\mathbf{R})}{\partial \mathbf{R}}\{E^{LS}_{U\text{-}BS}(\mathbf{R}) - E^{HS}_{U}(\mathbf{R})\} \quad (19)$$

$$\mathbf{F}^{LS}_{AP\text{-}BS}(\mathbf{R}) = \frac{\partial^2 E^{LS}_{AP\text{-}BS}(\mathbf{R})}{\partial \mathbf{R}^2} = \{\alpha(\mathbf{R})\boldsymbol{F}^{LS}_{U\text{-}BS}(\mathbf{R}) - \beta(\mathbf{R})\boldsymbol{F}^{HS}_{U}(\mathbf{R})\} + 2\frac{\partial \alpha(\mathbf{R})}{\partial \mathbf{R}}\{\boldsymbol{G}^{LS}_{U\text{-}BS}(\mathbf{R}) - \boldsymbol{G}^{HS}_{U}(\mathbf{R})\} + \frac{\partial^2 \alpha(\mathbf{R})}{\partial \mathbf{R}^2}\{E^{LS}_{U\text{-}BS}(\mathbf{R}) - E^{HS}_{U}(\mathbf{R})\} \quad (20)$$

where $\mathbf{G}^{LS}_{U\text{-}BS}$ and $\mathbf{G}^{HS}_{U}$ are energy gradients of the U-BS and the HS states, respectively. Because the spin contamination in the HS state is usually negligible as mentioned above, $\langle \hat{S}^2 \rangle^{HS}_{U}$ can be regarded as a constant. Therefore $\partial\alpha(\mathbf{R})/\partial\mathbf{R}$ and $\partial^2\alpha(\mathbf{R})/\partial\mathbf{R}^2$ can be expressed by $\langle \hat{S}^2 \rangle$ values of U-BS and HS states and $\partial\langle \hat{S}^2 \rangle^{LS}_{U\text{-}BS}/\partial\mathbf{R}$ as follows

$$\frac{\partial \alpha(\mathbf{R})}{\partial \mathbf{R}} = \frac{\langle \hat{S}^2 \rangle^{HS}_{U} - \langle \hat{S}^2 \rangle^{LS}_{exact}}{(\langle \hat{S}^2 \rangle^{HS}_{U} - \langle \hat{S}^2 \rangle^{LS}_{U\text{-}BS})^2}\frac{\partial \langle \hat{S}^2 \rangle^{LS}_{U\text{-}BS}}{\partial \mathbf{R}} \quad (21)$$

$$\frac{\partial^2 \alpha(\mathbf{R})}{\partial \mathbf{R}^2} = \frac{2(\langle \hat{S}^2 \rangle^{HS}_{U} - \langle \hat{S}^2 \rangle^{LS}_{exact})}{(\langle \hat{S}^2 \rangle^{HS}_{U} - \langle \hat{S}^2 \rangle^{LS}_{U\text{-}BS})^3}\left(\frac{\partial \langle \hat{S}^2 \rangle^{LS}_{U\text{-}BS}}{\partial \mathbf{R}}\right)^2 + \frac{\langle \hat{S}^2 \rangle^{HS}_{U} - \langle \hat{S}^2 \rangle^{LS}_{exact}}{(\langle \hat{S}^2 \rangle^{HS}_{U} - \langle \hat{S}^2 \rangle^{LS}_{U\text{-}BS})^2}\frac{\partial^2 \langle \hat{S}^2 \rangle^{LS}_{U\text{-}BS}}{\partial \mathbf{R}^2} \quad (22)$$

For the geometry optimization, eqs 19 and 21 are necessary. In this paper, $\partial\alpha(\mathbf{R})/\partial\mathbf{R}$ and $\partial^2\alpha(\mathbf{R})/\partial\mathbf{R}^2$ values are calculated numerically as explained in the next section.

As explained above, this AP-opt method involves several inherent approximations. Here we summarize the approximations.

(A) For degeneracy of orbitals, the BS (approximation) method is introduced.

(B) For Heisenberg Hamiltonian, spin densities of the BS method are considered to be localized spins.

(C) For the AP method, the spin contamination in the HS state is considered to be negligible.

(D) For the AP-opt method, $\langle \hat{S}^2 \rangle^{LS}_{U\text{-}BS}$ values are approximately fitted to a second degree polynomial.

3. Computational Details

In order to calculate the AP gradient by using eq 19, we have to obtain total energies, energy gradients, $\langle \hat{S}^2 \rangle$ values of U-BS and HS states, and $\partial\langle \hat{S}^2 \rangle^{LS}_{U\text{-}BS}/\partial\mathbf{R}$. Although various ab initio programs can be utilized for a calculation of the energy gradients and so on, they do not give us $\partial\langle \hat{S}^2 \rangle^{LS}_{U\text{-}BS}/\partial\mathbf{R}$ values. So, we introduced a numerical procedure based on the univariate method to calculate those values.[25] According to the method, $\langle \hat{S}^2 \rangle^{LS}_{U\text{-}BS}$ values were calculated at $\mathbf{R}_i$, $\mathbf{R}_i + \delta\mathbf{R}_i$, and $\mathbf{R}_i - \delta\mathbf{R}_i$ ($i = 1-3N$, $N =$ the number of optimizing atoms) and fitted to a second-degree polynominal before the geometry optimization calculations. The $\partial\langle \hat{S}^2 \rangle^{LS}_{U\text{-}BS}/\partial\mathbf{R}$ functions obtained from the numerically fitted $\langle \hat{S}^2 \rangle^{LS}_{U\text{-}BS}$ functions for all degrees of freedom make it possible to estimate $\partial\alpha(\mathbf{R})/\partial\mathbf{R}$ values at coordinate $\mathbf{R}$ easily in the subsequent AP optimization routine by substituting calculated $\langle \hat{S}^2 \rangle$ values of U-BS and HS states for eq 21 at each coordinate. The $\delta\mathbf{R}_i$ values were empirically determined as 0.05 Å, 0.5°, and 0.5° for distances, angles, and dihedral angles, respectively,[21,22] The AP optimization was carried out using our own program. All components of eqs 19 and 21 except for $\partial\langle \hat{S}^2 \rangle^{LS}_{U\text{-}BS}/\partial\mathbf{R}$ were calculated by using GAUSSIAN98 at each

TABLE 1: Optimized Structural Parameters of CH_2 by Spin-Symmetry Adapted (SA), Broken-Symmetry (BS), and Approximately Spin Projected (AP) Methods[d]

	r_{CH}[a]				θ_{HCH}[b]			
	SA	BS	AP	($^3B_1$)	SA	BS	AP	($^3B_1$)
				STO-3G				
HF	1.123	1.100	1.121	(1.082)	100.4	110.7	99.9	(125.5)
CID	1.155	1.098	1.152	(1.104)	97.8	129.1	98.8	(125.0)
CCD	1.157	1.092	1.152	(1.105)	97.7	143.6	99.6	(125.0)
MP2	1.144	1.116	1.142	(1.095)	98.2	109.2	97.5	(124.8)
MP3	1.154	1.123	1.151	(1.100)	97.5	109.0	97.1	(124.7)
MP4(SDQ)	1.158	1.126	1.154	(1.103)	97.3	109.4	97.2	(124.7)
B3LYP	1.154	1.124	1.142	(1.099)	97.1	108.4	99.9	(126.2)
				6-31G*				
HF	1.097	1.083	1.098	(1.071)	103.1	115.5	102.9	(130.7)
CID	1.114	1.091	1.112	(1.081)	101.6	119.7	101.9	(131.8)
CCD	1.116	1.087	1.113	(1.082)	101.7	125.1	102.4	(132.0)
MP2	1.109	1.091	1.109	(1.077)	102.0	114.7	100.9	(131.6)
MP3	1.109	1.094	1.112	(1.080)	102.0	114.9	101.0	(131.8)
MP4(SDQ)	1.117	1.096	1.114	(1.081)	101.2	115.0	101.0	(131.9)
B3LYP	1.120	1.100	1.113	(1.082)	100.3	112.9	103.2	(133.1)
CASSCF(2,2)	1.097				102.9			
CASSCF(6,6)	1.124				100.9			
MRMP2(2,2)	1.109				102.0			
MRMP2(6,6)	1.122				101.1			
				6-311++G**				
HF	1.098	1.084	1.099	(1.072)	103.6	116.4	103.4	(132.0)
CID	1.112	1.093	1.106	(1.081)	101.6	117.7	101.8	(132.9)
CCD	1.114	1.091	1.107	(1.082)	101.6	120.7	102.5	(132.9)
MP2	1.110	1.093	1.110	(1.079)	101.8	114.8	100.6	(132.5)
MP3	1.113	1.095	1.112	(1.081)	101.3	114.6	100.5	(132.7)
MP4(SDQ)	1.115	1.097	1.114	(1.082)	101.2	114.7	100.3	(132.8)
B3LYP	1.114	1.096	1.109	(1.080)	101.5	114.6	103.8	(135.5)
exptl[c]		1.107		(1.077)		102.4		(134.0)

[a] In angstroms. [b] In degrees. [c] In refs 28 and 29 for singlet and triplet states, respectively. [d] Optimized parameters of the $^3B_1$ state by unrestricted method are also written in parentheses.

coordinate.[26] Convergence criteria for the optimization were 0.00045 and 0.0018 au for an energy gradient and a displacement for all geometry optimizations, respectively. We note that the first-order corrected (U-BS MP2 level) $\langle \hat{S}^2 \rangle$ values are used for the AP optimization of MP3 and MP4 methods. All calculations about SA and BS methods are also carried out with GAUSSIAN98 except for CASSCF and MRMP calculations that are carried out by GAMESS.[27]

4. Calculated Results

The methylene molecule has two valence orbitals as explained above and has two spins in those orbitals. Those two orbitals are spatially orthogonal and energetically quasi-degenerate. The ground state of methylene is a triplet $^3B_1$ state, and a singlet $^1A_1$ state is the first excited state. Cramer et al. graphically explained the wave functions of the $^1A_1$ state with SA and U-BS methods well, as illustrated in parts a and b of Figure 1.[5] The SA method such as RHF considers only one configuration although the BS wave function consists of three components such as the lower singlet state, the two-electron excited singlet state, and the triplet state. The existence of the triplet component is the origin of the spin contamination error in this system.

Both $^1A_1$ and $^3B_1$ methylene molecules have bent structures, but the experimental data indicate a large structural difference between them. For example, experimental HCH angles (θ_{HCH}) of the singlet and the triplet states are 102.4° and 134.0°, respectively.[28,29] There have been many reports about the theoretical geometry optimization of this molecule. For example, Hargittai et al. summarized the calculated results about SA methods in their review.[30] However the report about the BS method still has been insufficient. As mentioned above, the BS method is a convenient substitute for CI and CAS methods, so we first optimize the geometry of the methylene by SA and BS methods. In order to elucidate a dependency of the spin contamination error on the calculation methods, HF, a configuration interaction method with all double substitutions (CID), a coupled-cluster method with double substitutions (CCD), several levels of Møller−Plesset energy correction methods (MP2, MP3, and MP4(SDQ)), and a hybrid DFT (B3LYP) method are examined. We also carry out CASSCF(n, n) and MRMP2(n, n) (n = 2, 6) methods. In addition, three basis sets with different levels such as small (STO-3G), middle (6-31G*) and large (6-311++G**) are used to examine the effects of the basis sets on the spin contamination error.

Calculated results are summarized in Table 1. In the case of the $^3B_1$ state, the optimized equilibrium structures reproduce the experimental values well by using 6-311++G**. In the case of the $^1A_1$ state, all SA results are in good agreement with the experimental values, while all the BS results overestimate the HCH angle. The difference in HCH angle between the U-BS values and experimental one is about 10−20°. The HCH angles of CI and CC methods are especially larger than MP and DFT methods. Therefore it is difficult to use the U-BS solution for the $^1A_1$ state without some corrections. On the other hand, by applying the AP method to the BS solution, the error is drastically improved and the optimized structural parameters came in good agreement with experimental ones. The difference in the optimized HCH angle between the BS and the AP method,

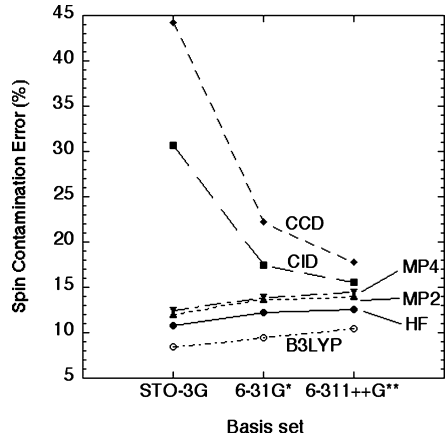

Figure 2. Basis set dependency of the spin contamination error by each method.

i.e., the spin contamination error, is about 10−20°. Those results strongly insist that the spin contamination is a serious problem in the structural optimization of the $^1A_1$ state and the AP method can successfully remove it. Interestingly, the optimized structural parameters obtained by the AP-UHF method are almost the same as the CASSCF(2,2) ones. This means that two-electron excitation involved in the AP method approximates the (2,2) active space well. The HCH angle becomes smaller by the use of larger CAS space such as CASSCF(6,6) or by adding the dynamical correlation correction such as MRMP2(2,2) and MRMP2(6,6). The result of the spin projected MP4 (AP MP4(SDQ)) successfully reproduced the MRMP2(6,6) result, indicating that the AP method plus dynamical correlation correction is a promising approach.

Next, we examine the basis set dependency of the spin contamination error. In order to estimate the error quantitatively, the percentage of the error is calculated by

$$\text{Error}[\%] = \frac{\theta_{\text{HCH}}(\text{BS}) - \theta_{\text{HCH}}(\text{AP})}{\theta_{\text{HCH}}(\text{AP})} \times 100 \qquad (23)$$

where $\theta_{\text{HCH}}(\text{X})$ is the optimized HCH angle by method X (X = BS or AP). The results are illustrated in Figure 2. The error depends on the basis sets, but the tendencies of each method are classified into two types. In the case of HF, MP, and DFT methods, for example, the error slightly increases as the basis set becomes larger, while the tendency is opposite in the case of CC and CI methods. In other words, we must pay attention to the spin contamination error if U-BS CCD and U-BS CID methods are used for similar systems with a small basis set.

Finally, we examined the energy splitting between singlet $^1A_1$ and triplet $^3B_1$ states (ST gap). The ST gap (ΔE_{ST}) is calculated from the difference in total energies at stationary points of singlet and triplet states, respectively

$$\Delta E_{\text{ST}}(\text{X}) = E_{\text{S}}(\text{X}) - E_{\text{T}}(\text{X}) \qquad (24)$$

where $E_{\text{S}}(\text{X})$ and $E_{\text{T}}(\text{X})$ are total energies of $^1A_1$ and $^3B_1$ states calculated by method X, respectively. The calculated results are summarized in Table 2. The schematic views of calculated potential curves and $\Delta E_{\text{ST}}(\text{X})$ are also illustrated in Figure 3. The experimental ST gap energy is 0.39 eV,[31] but all restricted methods overestimate the ST gap energy showing the necessity of the static correlation correction. On the other hand, the BS

TABLE 2: ΔE_{ST} Values[a] calculated by SA, BS, and AP Methods and $\Delta\Delta E_{\text{ST}}$ Values[a]

	ΔE_{ST}(SA)	ΔE_{ST} (BS)	ΔE_{ST} (AP)	$\Delta\Delta E_{\text{ST}}$ (SA-AP)	$\Delta\Delta E_{\text{ST}}$ (BS-AP)
			STO-3G/		
HF	1.74	0.96	1.36	0.38	−0.40
CID	1.13	0.62	1.08	0.05	−0.46
CCD	1.08	0.36	1.05	0.03	−0.69
MP2	1.38	0.87	1.19	0.18	−0.32
MP3	1.23	0.83	1.13	0.10	−0.30
MP4(SDQ)	1.17	0.81	1.10	0.06	−0.29
B3LYP	0.79	0.35	0.36	0.44	−0.01
			6-31G*/		
HF	1.34	0.71	0.99	0.35	−0.28
CID	0.76	0.50	0.63	0.13	−0.13
CCD	0.70	0.45	0.68	0.02	−0.23
MP2	0.91	0.60	0.80	0.11	−0.20
MP3	0.80	0.56	0.73	0.07	−0.17
MP4(SDQ)	0.75	0.54	0.71	0.05	−0.16
B3LYP	0.59	0.27	0.26	0.33	0.01
			6-311++G**		
HF	1.24	0.66	0.92	0.33	−0.26
CID	0.64	0.45	0.58	0.05	−0.14
CCD	0.56	0.41	0.55	0.01	−0.14
MP2	0.76	0.53	0.68	0.08	−0.14
MP3	0.64	0.49	0.60	0.04	−0.11
MP4(SDQ)	0.61	0.47	0.57	0.03	−0.10
B3LYP	0.53	0.25	0.24	0.29	0.01
exptl[b]		0.39			

[a] In eV. [b] In ref.[31]

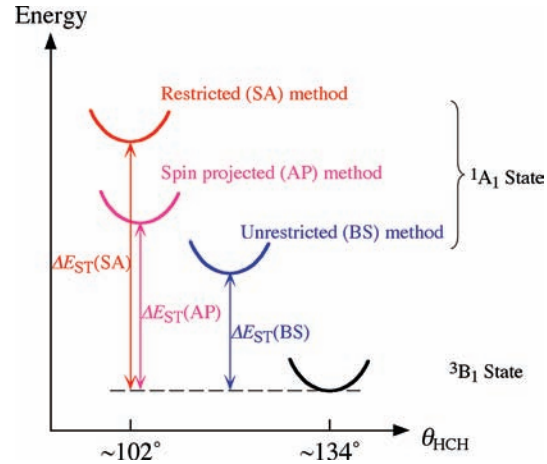

Figure 3. Schematic view of calculated potential surfaces and single−triplet energy splitting (ΔE_{ST}) of SA, BS, and AP methods.

method stabilizes the singlet energy too much by both static correlation correction and the contamination of the triplet state. The smaller ST gap of the BS method seems to be better than the SA method; however the singlet energy becomes slightly unstable by eliminating the triplet state. In the case of the post-HF methods, the difference between ΔE_{ST}(AP) and ΔE_{ST}(SA), namely

$$\Delta\Delta E_{\text{ST}}(\text{SA-AP}) = \Delta E_{\text{ST}}(\text{AP}) - \Delta E_{\text{ST}}(\text{SA}) \qquad (25)$$

becomes small in comparison with HF method and its order is less than 10^{-1} eV. This result indicates that the static correlation is well corrected even by the SA-based post-HF methods in terms of the ST gap energy. On the other hand, the difference between ΔE_{ST}(AP) and ΔE_{ST}(BS)

$$\Delta\Delta E_{ST}(\text{BS-AP}) = \Delta E_{ST}(\text{AP}) - \Delta E_{ST}(\text{BS}) \quad (26)$$

is not negligible in all methods except for the B3LYP method. In other words, a dominant factor of the *extra*-stabilization energy of the BS method originates in the triplet contamination. The energy order of the excess stabilization by the contamination is estimated to be 10^{-1} eV.

5. Conclusion

In this paper, we indicate that the spin contamination causes a serious error in geometry optimization of biradical systems. To our knowledge, this is the first report about a quantitative analysis of the spin contamination error in the U-BS solution of the CH_2 molecule. The estimated error is not negligible, and it may mislead the conclusion.[24] In this way, one must pay attention to the spin contamination error in the optimized geometry if the U-BS and the HS states have different potential surfaces. There are many large biradical systems such as polymetal complexes, bioinorganic systems, and so on. Because their properties and reactivity are sometimes sensitive to the geometry, a method to correct the spin contamination with a simple and easy way is necessary for the ab initio calculation of those systems. In this paper, we could demonstrate that the AP-opt method eliminates the spin contamination error in the optimized geometry of biradicals. From those points of view, we conclude that the AP method is one of the effective tools for the theoretical calculations of the singlet biradical and related species.

On the other hand, the AP method is also effective in the investigation of the chemical reaction because a homolytic bond cleavage causes the biradical state. In Figure S1 of the Supporting Information, the spin contamination error in the total energy of H_2 molecule is depicted at several bond distances. In the covalent bond region, there are no spin contamination errors because the BS method corresponds to the SA method. However, the error suddenly increases around the bifurcation point between the SA and the U-BS states (∼1.3 Å). Therefore, we also have to take care about the spin contamination if the transition state or intermediate state is close to the bifurcation point, and the AP method is also effective in such situations.

Acknowledgment. This work has been supported by Grants-in-Aid for Scientific Research (KAKENHI) (Nos. 19750046, 19350070, 18350008) from the Japan Society for the Promotion of Science (JSPS) and that on Priority Areas (No. 19029028) from the Ministry of Education, Culture, Sports, Science and Technology (MEXT).

Supporting Information Available: Figures showing potential curves of H2 by the SA and BS methods and the spin contamination error in the total energy of the BS method. This information is available free of charge via the Internet at http://pubs.acs.org.

References and Notes

(1) Nakatsuji, H. *Phys. Rev. Lett.* **2004**, *93*, 030403. (b) Nakatsuji, H.; Nakashima, H.; Kurokawa, Y.; Ishikawa, A. *Phys. Rev. Lett.* **2007**, *99*, 240402.

(2) Ryde, U.; Olsson, H. M. *Int. J. Quantum Chem.* **2001**, *81*, 335.

(3) Comba, P.; Liedós, A.; Maseras, F.; Remenyi, R. *Inorg. Chim. Acta* **2001**, *324*, 21.

(4) Noodleman, L.; Han, W.-G. *J. Biol. Inorg. Chem.* **2006**, *11*, 674.

(5) Cremer, D. *Mol. Phys.* **2001**, *99*, 1899.

(6) Roos, B. O.; Taylor, P. R.; Siegbahn, P. E. M. *Chem. Phys.* **1980**, *48*, 157.

(7) Andersson, K.; Malmqvist, P. -Å.; Roos, B. O.; Sadlej, A. J.; Wolinski, K. *J. Chem. Phys.* **1990**, *94*, 5483.

(8) Hirao, K. *Chem. Phys. Lett.* **1992**, *190*, 374.

(9) Löwdin, P.-O. *Phys. Rev.* **1955**, *97*, 1509.

(10) Lykos, P.; Pratt, G. W. *Rev. Mod. Phys.* **1963**, *35*, 496.

(11) Yamaguchi, K. In *Self-Consistent Field Theory and Applications*, ed. Carbo, R., Klobukowski, M., Eds.; Elsevier: Amsterdam, 1990; p 727.

(12) Yamaguchi, K.; Kawakami, T.; Takano, Y.; Kitagawa, Y.; Yamashita, Y.; Fujita, H. *Int. J. Quantum Chem.* **2002**, *90*, 370.

(13) Hehre, W. J.; Random, L.; von Schleyer P. R.; Pople, J. A. *Ab Initio Molecular Orbital Theory*; Wiley: New York, 1986.

(14) Szabo, A.; Ostlund, N. S. *Modern Quantum Chemistry*; Dover Publications, Inc.: New York, 1996.

(15) Mayer, I. *Advances in Quantum Chemistry*; Löwdin, P.-O., Ed.; Academic Press, Inc.: New York, 1980; Vol. 12, p189.

(16) Löwdin, P.-O. *Rev. Mod. Phys.* **1964**, *36*, 966.

(17) Yamaguchi, K.; Takahara, Y.; Fueno, T.; Houk, K. N. *Theor. Chim. Acta* **1988**, *73*, 337.

(18) Yamaguchi, K.; Okumura, M.; Mori, W. *Chem. Phys. Lett.* **1993**, *210*, 201.

(19) Yamanaka, S.; Okumura, M.; Nakano, M.; Yamaguchi, K. *J. Mol. Struct.: THEOCHEM* **1994**, *310*, 205.

(20) Helgaker, T.; Jørgensen, P. *Advances in Quantum Chemistry*; Löwdin, P.-O., Ed.; Academic Press, Inc.: New York, 1980; Vol. 19.

(21) Kitagawa, Y.; Saito, T.; Ito, M.; Shoji, M.; Koizumi, K.; Yamanaka, S.; Kawakami, T.; Okumura, M.; Yamaguchi, K. *Chem. Phys. Lett.* **2007**, *442*, 445 We note that the minus sign of eq 9 in this reference should read plus, as displayed in eq 21.

(22) Kitagawa, Y.; Saito, T.; Ito, M.; Nakanishi, Y.; Shoji, M.; Koizumi, K.; Yamanaka, S.; Kawakami, T.; Okumura, M.; Yamaguchi, K. *Int. J. Quantum Chem.* **2007**, *107*, 3094.

(23) Kitagawa, Y.; Saito, T.; Nakanishi, Y.; Kataoka, Y.; Shoji, M.; Koizumi, K.; Kawakami, T.; Okumura, M.; Yamaguchi, *Int. J. Quantum Chem.* **2009**, *109*, 3632.

(24) Saito, T.; Kitagawa, Y.; Shoji, M.; Nakanishi, Y.; Ito, M.; Kawakami, T.; Okumura, M.; Yamaguchi, K. *Chem. Phys. Lett.* **2008**, *456*, 76.

(25) Reach, A. R. *Molecular Modeling—Principles and Applications*, 2nd ed.; Pearson Education Ltd.: Harlow, Essex, U.K., 1996; Chapter 5.

(26) Frisch, M. J.; Trucks, G. W.; Schlegel, H. B.; Scuseria, G. E.; Robb, M. A.; Cheeseman, J. R.; Zakrzewski, V. G.; Montgomery, J. A., Jr.; Stratmann, R. E.; Burant, J. C.; Dapprich, S.; Millam, J. M.; Daniels, A. D.; Kudin, K. N.; Strain, M. C.; Farkas, O.; Tomasi, J., Barone, V.; Cossi, M., Cammi, R.; Mennucci, B., Pomelli, C.; Adamo, C., Clifford, S.; Ochterski, J., Petersson, G. A.; Ayala, P. Y.; Cui, Q.; Morokuma, K.; Malick, D. K.; Rabuck, A. D.; Raghavachari, K.; Foresman, J. B.; Cioslowski, J.; Ortiz, J. V.; Stefanov, B. B.; Liu, G.; Liashenko, A.; Piskorz, P.; Komaromi, I.; Gomperts, R.; Martin, R. L.; Fox, D. J.; Keith, T.; Al-Laham, M. A.; Peng, C. Y.; Nanayakkara, A.; Gonzalez, C.; Challacombe, M.; Gill, P. M. W.; Johnson, B.; Chen, W.; Wong, M. W.; Andres, J. L.; Gonzalez, C.; Head-Gordon, M.; Replogle, E. S.; Pople J. A. *Gaussian 98*; Gaussian, Inc.: Pittsburgh, PA, 1998.

(27) Schmidt, M. W.; Baldridge, K. K.; Boatz, J. A.; Elbert, S. T.; Gordon, M. S.; Jensen, J. H.; Koseki, S.; Matsunaga, N.; Nguyen, K. A.; Su, S. J.; Windus, T. L.; Dupuis, M.; Montgomery, J. A. GAMESS Ver.22. *J. Comput. Chem.* **1993**, *14*, 1347.

(28) Petek, H.; Nesbitt, D. J.; Darwin, D. C.; Ogilby, P. R.; Moore, C. B.; Ramsay, D. A. *J. Chem. Phys.* **1989**, *91*, 6566.

(29) Bunker, P. R.; Jensen, P.; Kraemer, W. P.; Beardsworth, R. *J. Chem. Phys.* **1986**, *85*, 3724.

(30) Hargittai, M.; Schults, G.; Hargittai, I. *Russ. Chem. Bull.* **2001**, *50*, 1903.

(31) Leopold, D. G.; Murray, K. K.; Stevens, A. E.; Lineberger, W. C. *J. Chem. Phys.* **1985**, *83*, 4849.

JP905125G